Confinement of Surface State Electrons in Fabry-Pérot Resonators

L. Bürgi, O. Jeandupeux, A. Hirstein, H. Brune, and K. Kern

Institut de Physique Expérimentale, Ecole Polytechnique Fédérale de Lausanne, CH-1015 Lausanne, Switzerland

(Received 7 August 1998)

Ag(111) surface state electrons have been confined in symmetric and asymmetric Fabry-Pérot resonators formed by two atomically parallel step edges. The local density of states in the resonators has been measured by means of low-temperature scanning tunneling spectroscopy and can perfectly be explained with a simple Fabry-Pérot-like model. The energy dependent reflection amplitudes and scattering phase shifts of the different kinds of Ag(111) step edges have been determined with high accuracy. The model character of the resonators opens up quantitative electron scattering experiments at test structures brought into the resonator. [S0031-9007(98)07883-1]

PACS numbers: 61.16.Ch, 72.10.Fk, 73.20.Dx

Quantum interference of electrons in low-dimensional structures has attracted much interest in recent years. Elegant methods have been developed to probe the quantum-mechanical probability density distribution of electrons in semiconductor heterostructures [1,2] and in Shockley-type surface states of metals [3–6]. In particular, the real space visualization of the local density of states (LDOS) of surface state electrons by means of scanning tunneling microscopy/spectroscopy (STM/STS) has created a lot of excitement [7,8]. Surface state electrons may be confined laterally by steps and in cages assembled from adsorbates, leading to tantalizing interference patterns in their LDOS [4,7–10]. The confinement of 2D electrons and the mapping of its LDOS with STS make it possible to use the surface as a quantum laboratory. This has been employed to illustrate solutions of the Schrödinger equation [7], and attempts were made to visualize quantum chaos [9]. Challenges in surface state electron confinement are the quantification and possibly improvement of the scattering properties of the confining structures, and the construction of quantum resonators which could be used to study electronic properties of nanosized structures introduced into them, much as in optics.

The most obvious choice for such a resonator is a set of two perfectly straight and parallel steps. This geometry enables the description of the LDOS in the resonator through analogy with a Fabry-Pérot etalon known from optics. Electron scattering at parallel step arrangements has been investigated earlier [4,8,11]; however, steps were treated as real hard-wall or δ potentials, and hence the absorption processes at step edges due to bulk coupling were disregarded. In this Letter we present measurements of the LDOS in symmetric and asymmetric quantum resonators consisting of pairs of ascending and ascending/descending close-packed steps on Ag(111). We introduce a Fabry-Pérot model establishing a direct correlation of the LDOS in the resonator with the step reflection amplitude, r, and scattering phase, φ. The model reveals the different roles of φ and r on peak positions and peak broadening of the quantized states and enables the determination of the full scattering properties of the different kinds of monatomic steps on Ag(111). We present the first measurements of the energy dependence of the reflection amplitude.

The experiments were performed with a homebuilt low-temperature UHV STM. The Ag(111) surface has been cleaned by sputter-anneal cycles. All measurements have been performed at $T = 4.9$ K, with a tungsten tip and the bias voltage V applied to the sample.

Figure 1 illustrates the quantum resonators bound by $\langle 1\bar{1}0\rangle$-oriented monatomic steps. The symmetric resonator consists of two ascending steps, one is of type A ($\{100\}$ facet) and the other one of type B ($\{111\}$ facet). The asymmetric resonator is formed either by (A_{desc}, A_{asc}) or (B_{desc}, B_{asc}) steps [see also profiles in Figs. 2(a) and 3(a)]. Because of the translational symmetry along the resonators, their LDOS depends only on the x direction perpendicular to the resonator. In the following the variable x is assumed to quantify the distance from the left step edge. In this direction conductance maps $dI/dV(E, x)$ were recorded by measuring $dI/dV(E)|_x$ along a constant current line scan. $dI/dV(E)|_x$ has been acquired under open feedback-loop conditions by conventional lock-in technique with a 1.2 kHz modulation of the bias by typically 5 mV rms. The tip height z has been stabilized at a relatively large bias voltage. Under these conditions, and since the conductance spectra have been measured for a narrow energy window around E_{F}, $dI/dV(E, x)$ can directly be interpreted in terms of the surface LDOS [12].

Figure 2(b) shows a dI/dV map of a 56 Å wide symmetric resonator (the ordinate shows E with respect to E_{F}). The quantum nature of the LDOS due to electron confinement is evident. The "ground state" is located at -30 meV, the first "excited state" with one node at 65 meV, and the second excited state with two nodes at 220 meV. Around 290 meV, there is a location independent enhancement of dI/dV due to an enhanced tip DOS at this energy.

To derive the scattering properties of the step edges from the measured LDOS in the resonators, we model the steps by semitransparent mirrors with coherent reflection amplitudes r_ℓ, r_{r}, and coherent reflection phase shifts φ_ℓ, φ_{r}, where ℓ and r denote the left- and right-hand

 0031-9007/98/81(24)/5370(4)$15.00

steps, respectively. The mirrors are by definition located at the midheight points in the constant current line scan of the step. The electrons between the steps are freelike [5,6,13]. The electron-electron interaction in these two-dimensional surface states is screened by the underlying bulk electrons [14]. In analogy to the Fabry-Pérot interferometer the surface LDOS ρ_s in the resonator for freelike surface state electrons is readily calculated to yield

$$\rho_s(E,x) = \rho_b + \frac{L_0}{\pi}\int_0^k dq\,\frac{1}{\sqrt{k^2-q^2}}\,\frac{1}{1+r_\ell^2 r_r^2 - 2r_\ell r_r\cos(2qa+\varphi_\ell+\varphi_r)} \times\{(1-r_\ell^2)[1+r_r^2+2r_r\cos(2q(x-a)-\varphi_r)] + (1-r_r^2)[1+r_\ell^2+2r_\ell\cos(2qx+\varphi_\ell)]\},$$

where $k=\sqrt{2m^*(E-E_0)/\hbar^2}$, a is the width of the resonator, $L_0 = m^*/(\pi\hbar^2)$ is the density of states of a free 2D electron gas, and ρ_b is the bulk contribution to the surface LDOS. The effective mass $m^* = (0.40 \pm 0.01)m_e$ and the surface state band edge energy $E_0 = (-65 \pm 3)$ meV for Ag(111) have been determined previously, as well as $\rho_b = 0.57L_0$ [13]. This reduces the number of free parameters (apart from a proportionality factor between dI/dV and ρ_s) to four, namely, the four step reflection parameters. Note that for the limiting case $r_\ell,\ r_r \to 0$, $\rho_s(E,x)$ reproduces the LDOS of a 2D free electron gas. On the other hand, when $r_\ell,\ r_r \to 1$, $\varphi_\ell,\ \varphi_r \to -\pi$, it collapses to the hard wall potential model with sharp nonanalytical rises in the LDOS at energies $E_n = \hbar^2/(2m^*)k_n^2$, where $k_n a = (n+1)\pi$ with $n = 0, 1, \ldots$, followed by a $1/\sqrt{E-E_n}$ decay due to the fact that the electrons are free parallel to the steps [see Fig. 4(a), dashed line].

The energies as well as the lateral positions at which the maxima in $\rho_s(E,x)$ appear depend strongly on the phase shifts $\varphi_\ell,\ \varphi_r$, and only weakly on the amplitudes $r_\ell,\ r_r$. On the other hand, the broadening of the peaks of $\rho_s(E)|_x$ and the oscillation amplitude of $\rho_s(x)|_E$ are determined by the reflection amplitudes $r_\ell,\ r_r$. Hence, due to their different roles, φ and r can be determined separately. Furthermore, differences in scattering properties on the left-hand and on the right-hand sides directly show up in the LDOS patterns inside the resonator: the maxima shift to either side of the resonator if $\varphi_\ell \neq \varphi_r$ and asymmetric amplitudes result from $r_\ell \neq r_r$.

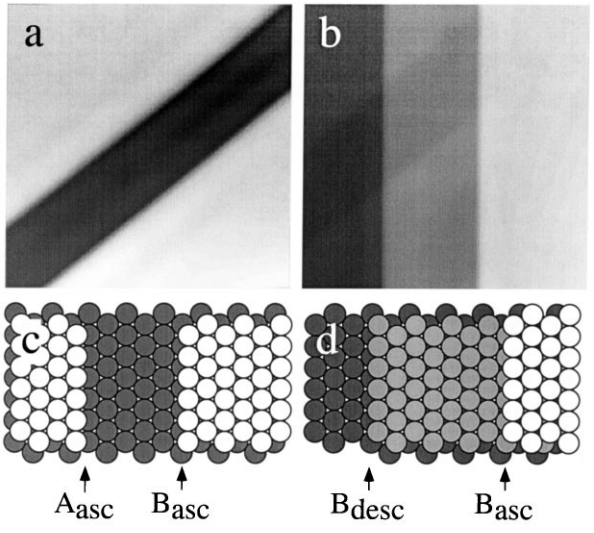

FIG. 1. Constant current images ($V = 100$ mV, $I = 1$ nA) show (a) a 56 Å wide symmetric resonator (215 Å × 215 Å) and (b) a 104 Å wide asymmetric resonator (311 Å × 311 Å). Hard sphere models for symmetric and asymmetric resonators are sketched in (c) and (d), respectively.

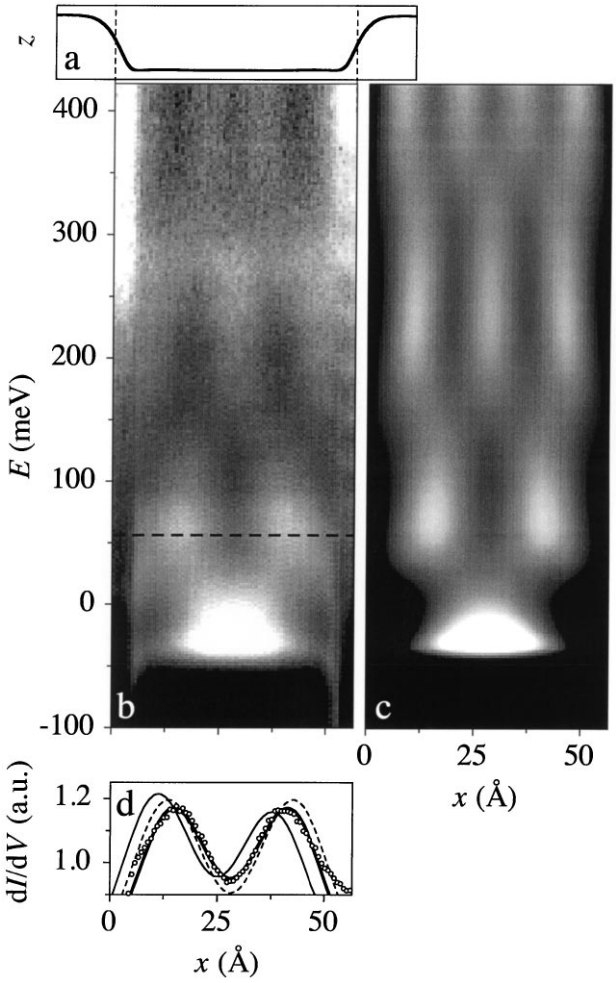

FIG. 2. (a) Constant current line scan over 56 Å wide symmetric resonator taken at $V = 303$ mV and $I = 2$ nA. (b) Corresponding differential conductance map. (c) Model calculation of $\rho_s(E,x)$ using the parameters: $a = 56$ Å, $\varphi_\ell = \varphi_r = -\pi$, $r_\ell = r_r = r_{asc}(E)$ of Fig. 4. (d) Constant energy cut through (b) at $E = 56.3$ meV (see dashed line) plotted as open circles. The thick line displays $\rho_s(x)|_{E=56.3\,\mathrm{meV}}$ for $\varphi_\ell = \varphi_r = -\pi$. The sensitivity of the peak position to the choice of the phase shifts is demonstrated by the thin full ($\varphi_\ell = -\frac{3}{4}\pi,\ \varphi_r = -\frac{5}{4}\pi$) and the dashed line ($\varphi_\ell = \varphi_r = -\frac{3}{4}\pi$). $r_\ell = r_r = 0.35$ for all three curves.

By carefully inspecting the measured LDOS map for the symmetric resonator in Fig. 2(b) we observe no significant asymmetry in peak positions and amplitudes, leading to the conclusion that *A and B steps on Ag(111) reflect the surface state electrons in the very same way*, in contrast to previous results on Au(111) [6]. Thus, $\varphi_{A_{\rm asc}} = \varphi_{B_{\rm asc}} =: \varphi_{\rm asc}$ and $r_{A_{\rm asc}} = r_{B_{\rm asc}} =: r_{\rm asc}$. The positions of the maxima of dI/dV reveal the phase shift with high accuracy: $\varphi_{\rm asc} = -\pi \pm 0.3$, independent of energy [see, e.g., Fig. 2(d)]. The only remaining free parameter needed to fully describe the symmetric resonator, $r_{\rm asc}$, was now determined by fitting $dI/dV(x)|_E$ with $\rho_{\rm s}(x)|_E$ for all energies. The energy dependent reflection amplitudes for ascending steps, $r_{\rm asc}(E)$, resulting from these fits is shown in Fig. 4(b) (open symbols) [15]. The LDOS map calculated with the model in Fig. 2(c) agrees well with the measured LDOS concerning peak positions, peak broadening, and evolution of the maxima.

Our finding that ascending *A* and *B* steps have identical scattering properties strongly suggests that electron scattering will be identical for the two microfacets also at descending steps. Under this assumption, the asymmetric resonator can now be described with only two remaining free parameters within the Fabry-Pérot model, i.e., $\varphi_{\rm desc}$ and $r_{\rm desc}$. Figure 3(b) displays the measured $dI/dV(E,x)$ for a 104 Å wide asymmetric resonator. In contrast to the symmetric resonator the maxima evolution is now clearly asymmetric. Maxima evolve from bottom right to top left, indicative for the different scattering behavior of descending and ascending steps. The phase shift $\varphi_{\rm desc}$ is again determined by comparing the measured position of the nth maximum with E_n of the model. The energies

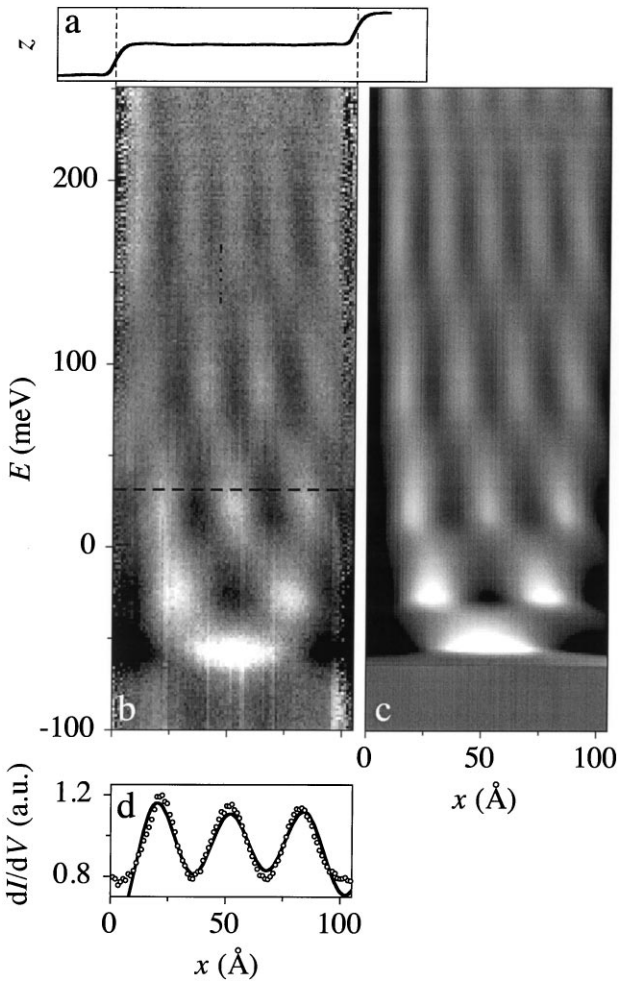

FIG. 3. (a) Constant current line scan over 104 Å wide asymmetric resonator taken at $V = 115$ mV and $I = 1$ nA. (b) Corresponding differential conductance map. (c) Model $\rho_s(E,x)$ with $a = 104$ Å, $\varphi_\ell = \varphi_{\rm r} = -\pi$, $r_\ell = r_{\rm desc}(E)$, and $r_{\rm r} = r_{\rm asc}(E)$ of Fig. 4 [line-by-line constants have been subtracted horizontally to enhance contrast in (b) and (c)]. (d) A constant energy cut of (b) at $E = 31.5$ meV (see dashed line) is plotted as open circles. The line depicts $\rho_{\rm s}(x)|_{E=31.5\ {\rm meV}}$ for $\varphi_\ell = \varphi_{\rm r} = -\pi$, $r_\ell = 0.70$, and $r_{\rm r} = 0.37$.

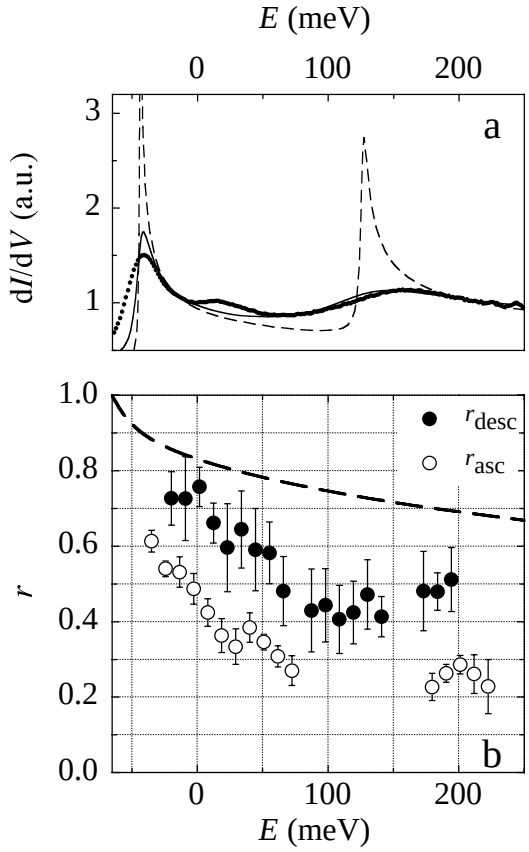

FIG. 4. (a) Measured dI/dV spectrum in the center of a 67 Å wide asymmetric resonator (dots) showing peak broadening due to the reduced reflectivity of the boundaries. The shoulder around 25 meV is due to the finite tip width which thus collects signal from the $n = 1$ maxima even in the center. The full line displays the LDOS $\rho_{\rm s}(E)|_{x=a/2}$ with $\varphi_{\rm desc} = \varphi_{\rm asc} = -\pi$ and $r_{\rm desc}(E)$ and $r_{\rm asc}(E)$ given by the measured values represented in (b). The dashed line shows for comparison the quasi-ideal resonator ($r = 0.95$). (b) Energy dependent reflection amplitudes for descending and ascending step edges on Ag(111) determined as described in the text. For qualitative comparison the calculated reflection amplitude of two missing rows on Cu(111) is shown as a dashed line [17]. (The curve was shifted by 375 meV to adjust the surface state band edges.)

of the confined eigenstates for 57, 67, 104, and 210 Å wide asymmetric resonators scale with $(n + 1)^2/a^2$, as in the case of ideal confinement. Their absolute values consistently yield $\varphi_{\mathrm{desc}} = -\pi \pm 0.4$. We are again left with only one parameter, and can extract $r_{\mathrm{desc}}(E)$ from fitting $dI/dV(x)|_E$ for asymmetric resonators of different widths. The result is depicted in Fig. 4(b). $r_{\mathrm{desc}}(E)$ is by about a factor of 2 larger than $r_{\mathrm{asc}}(E)$, in accordance with oscillation amplitudes in constant current line scans left and right from steps [13]. Figure 3(c) shows the model LDOS with reflection phase shifts $-\pi$ and the amplitudes $r_{\mathrm{desc}}(E)$ and $r_{\mathrm{asc}}(E)$ from Fig. 4. There is excellent agreement between the measured conductance map and our simple Fabry-Pérot model. Note how well the asymmetric evolution of the peak amplitudes is explained by the different reflectivities. The amplitude asymmetry is clearly visible in the constant energy line cut in Fig. 3(d).

Our finding of a common phase shift of $-\pi$ for the four different kinds of steps indicates a net repulsive interaction of surface state electrons with steps on Ag(111) [4,6]. Together with the strongly reduced reflection amplitudes the phase shifts of $-\pi$ imply considerable absorption of surface state electrons at steps [16]. This is further supported by the fact that the measured LDOS outside the resonator cannot be distinguished from the LDOS of a single step edge and thus the resonator is decoupled from its surrounding through the absorptive processes. The absorption process is most likely coupling to bulk states since the step allows for mixing of the orthogonal surface and bulk states. The difference between $r_{\mathrm{desc}}(E)$ and $r_{\mathrm{asc}}(E)$ is rationalized in geometric terms; i.e., the surface state wave functions show a stronger overlap with bulk states at ascending steps, leading to a stronger coupling and hence absorption for this step type. Figure 4(a) clearly shows that the enhanced level widths compared to a quasi-infinite hard wall model (see dashed line) can be rationalized only by reduced reflection amplitudes. We emphasize that reduced step reflection amplitudes are the dominant broadening mechanism above all other conceivable effects. Thermal broadening at 4.9 K and the bias modulation of $\approx$5 meV cannot account for the measured level widths. Electron lifetime broadening, e.g., due to electron-phonon or electron-electron coupling, can also be ruled out for the following reasons: the phase relaxation length of the Ag(111) surface state electrons at 4.9 K is much larger than the resonator widths for $E < 400$ meV [13], and the determined reflection amplitudes are independent of the resonator width. Finally, the finite tip width can be discarded since different tips have yielded the same results, and typical intermaxima distances of $\rho_s(x)|_E$ are large compared to typical tip radii.

The coupling of surface state electrons to the underlying bulk states is the most important process in causing imperfection of electron confinement. Former 1D Kronig-Penney models, employed for vicinal surfaces, disregarded this coupling as well as the difference between ascending and descending steps yielding unrealistic scattering phases [4,11]. The coupling to bulk states was treated for scattering centers on Cu(111) [17,18], with the result of monotonically decreasing reflection amplitudes with increasing energy for different kinds of scatterers. The data reproduced in Fig. 4(b) are the first experimental confirmation of this prediction.

In conclusion, we have measured the LDOS in quantum resonators for surface state electrons realized by two parallel steps on a Ag(111) surface. The analogy to wave optics was employed to model the LDOS pattern in terms of the scattering properties of the resonator boundaries. The electron reflectivity is found to be independent of the crystallographic step structure (A/B) but depends on the step morphology (ascending/descending). With our method, $r(E)$ and φ can be quantified for any two parallel steps, enabling studies of electron scattering at modified (decorated) steps and providing insight into the scattering mechanism. In analogy to optics the quantum resonators can also be employed as a sensitive tool to probe the electron interaction with magnetic and nonmagnetic atoms and nanostructures introduced into them. Deviations of the conductance maps from the model LDOS could be detected with high precision and related to the interaction mechanism.

[1] J.-Y. Marzin and J.-M. Gérard, Phys. Rev. Lett. **62**, 2172 (1989).
[2] G. Salis *et al.*, Phys. Rev. Lett. **79**, 5106 (1997).
[3] T. C. Hsieh, T. Miller, and T.-C. Chiang, Phys. Rev. Lett. **55**, 2483 (1985).
[4] L. C. Davis *et al.*, Phys. Rev. B **43**, 3821 (1991).
[5] M. F. Crommie, C. P. Lutz, and D. M. Eigler, Nature (London) **363**, 524 (1993).
[6] Y. Hasegawa and P. Avouris, Phys. Rev. Lett. **71**, 1071 (1993).
[7] M. F. Crommie, C. P. Lutz, and D. M. Eigler, Science **262**, 218 (1993).
[8] P. Avouris and I.-W. Lyo, Science **264**, 942 (1994).
[9] E. J. Heller *et al.*, Nature (London) **369**, 464 (1994).
[10] J. Li *et al.*, Phys. Rev. Lett. **80**, 3332 (1998).
[11] O. Sánchez *et al.*, Phys. Rev. B **52**, 7894 (1995).
[12] G. Hörmandinger, Phys. Rev. B **49**, 13 897 (1994).
[13] O. Jeandupeux *et al.* (to be published).
[14] F. Stern, Phys. Rev. Lett. **18**, 546 (1967).
[15] Since the step electronic structure influences the spectra up to 8 Å off its midpoints [see Fig. 2(b)], only data outside this range were included in the fit. Influence of the measurement on the LDOS can be excluded since various stabilizing impedances showed identical differential conductance maps.
[16] Neglecting absorption and modeling the step by a real δ potential leads to the relation $r = 1/\sqrt{1 + \tan^2(\varphi + \pi)}$ [4], which is obviously not fulfilled in our case.
[17] G. Hörmandinger and J. B. Pendry, Phys. Rev. B **50**, 18 607 (1994).
[18] S. Crampin, M. H. Boon, and J. E. Inglesfield, Phys. Rev. Lett. **73**, 1015 (1994).